Unsteady mixed convection from a rotating cone in a rotating fluid due to the combined effects of thermal and mass diffusion

S. Roy *, D. Anilkumar

Department of Mathematics, Indian Institute of Technology Madras, Chennai 600 036, India

Received 11 July 2003; received in revised form 27 October 2003

Abstract

A semi-similar solution of an unsteady mixed convection flow over a rotating cone in a rotating viscous fluid has been obtained when the free stream angular velocity and the angular velocity of the cone vary arbitrarily with the time. Both the prescribed wall temperature and the prescribed heat flux conditions are considered in the present investigation. The non-linear coupled partial differential equations governing the mixed convection flow have been solved numerically using an implicit finite difference scheme in combination with the quasi-linearization technique. Numerical results are presented for the skin friction coefficients, Nusselt number and Sherwood number. The effects of various parameters on the velocity, temperature and concentration profiles are also reported here.
© 2003 Elsevier Ltd. All rights reserved.

Keywords: Mixed convection; Rotating cone; Semi-similar solution

1. Introduction

Convective heat transfer in rotating flows over a stationary or rotating cone is important for the thermal design of various types of industrial equipments such as rotating heat exchangers, spin stabilized missiles, canisters for nuclear waste disposal, nuclear reactor cooling system and geothermal reservoirs. The cooling of the nose-cone of re-entry vehicle by spinning the nose [1] may also be considered as another possible application of the present study. The system to be studied, shown schematically in Fig. 1, is a right circular cone rotating about its vertical axis of symmetry in a rotating viscous fluid. The rotational motion of the cone induces a circumferential velocity in the fluid through the action of

viscosity. Further, due to the action of the centrifugal force field, the fluid is impelled along the cone surface parallel to a cone ray, and to satisfy conservation of mass, fluid distant from the cone migrates towards it, replacing the fluid which has been centrifuged along the cone surface. If the cone surface and free stream fluid temperature differ, not only energy will be transferred to the flow but also density difference will exist. In a gravitational field these density differences result in an additional force(buoyancy force) besides that due to the viscous action or the centrifugal force field. In many practical circumstances of moderate flow velocities and large wall-fluid temperature differences, the magnitudes of buoyancy force and the centrifugal force are of comparable order and convective heat transfer process is considered as mixed convection.

The early works of Tien and Tsuji [2], and Koh and Price [3] present a theoretical analysis of the forced flow and heat transfer past a rotating cone and the influence of Prandtl number on the heat transfer on rotating non-isothermal disks and cones was described by Hartnett and Deland [4]. Also, the similarity solution of the mixed

---

* Corresponding author. Tel.: +91-44-2257-8492; fax: +91-44-2257-8470.

E-mail addresses: sjroy@iitm.ac.in (S. Roy), anil@math.net (D. Anilkumar).

URL: http://mat.iitm.ac.in/sjroy.

Nomenclature

C, D species concentration and mass diffusivity, respectively

C_{fx}, C_{fy} local skin friction coefficients in the x- and y-directions, respectively for PWT case

$\overline{C_{fx}}, \overline{C_{fy}}$ local skin friction coefficients in the x- and y-directions, respectively for PHF case

f, f_η, g dimensionless stream function, velocity components in x- and y-directions, respectively for PWT case

F, F_η, G dimensionless stream function, velocity components in x- and y-directions, respectively for PHF case

g^* acceleration due to gravity

Gr_1, Gr_2 Grashof numbers due to temperature and concentration distributions, respectively for PWT case

Gr_1^*, Gr_2^* Grashof numbers due to temperature and concentration distributions, respectively for PHF case

k thermal conductivity

L characteristic length

N, N^* ratio of the Grashof numbers for PWT and PHF cases, respectively

$Nu_x, \overline{Nu_x}$ local Nusselt numbers for PWT and PHF cases, respectively

Pr Prandtl number

Re_L Reynolds number based on length L

Re_x Reynolds number based on length x

$R(t^*)$ function of t^* with first order continuous derivative

$Sh_x, \overline{Sh_x}$ local Sherwood numbers for PWT and PHF cases, respectively

t, t^* dimensional and dimensionless times, respectively

T temperature

u, v, w velocity components in the x-, y- and z-directions, respectively

x, y, z distances measured along meridional section, circular section and normal to the cone surface, respectively

Greek symbols

α^* semi-vertical angle of the cone

α_1 ratio of the angular velocity of cone to the angular velocity of free stream

β, β^* volumetric coefficients of the thermal and concentration expansions, respectively

ϵ constant

η similarity variable

θ, ϕ dimensionless temperature and concentration, respectively for PWT

Θ, Φ dimensionless temperature and concentration, respectively for PHF

λ_1, λ_2 buoyancy parameters due to the temperature and concentration gradients, respectively for PWT case

λ_1^*, λ_2^* buoyancy parameters due to the temperature and concentration gradients, respectively for PHF case

μ dynamic viscosity

v kinematic viscosity

ρ density

Ω_1, Ω_2 angular velocity of the cone and the free stream fluid, respectively

$\Omega(= \Omega_1 + \Omega_2)$ composite angular velocity

Subscripts

i initial condition

0 value at the wall for $t^* = 0$

w, ∞ conditions at the wall and infinity, respectively

t, x, z denote the partial derivatives w.r.t. to these variables, respectively

convection from a rotating vertical cone in an ambient fluid was obtained by Hering and Grosh [5] for Prandtl number $Pr = 0.7$. In a further study, Himasekhar et al. [6] found the similarity solution of the mixed convection flow over a vertical rotating cone in an ambient fluid for a wide range of Prandtl numbers. Wang [7] has also obtained a similarity solution of boundary layer flows on rotating cones, discs and axisymmetric bodies with concentrated heat sources. Further, Yih [8] has presented non-similar solutions to study the heat transfer characteristics in mixed convection about a cone in saturated porous media. All these studies pertain to steady flows. In many practical problems, the flow could be unsteady due to the angular velocity of the spinning body which varies with time or due to the impulsive change in the angular velocity of the body or due to the free stream angular velocity which varies with time. The unsteady boundary layer flow of an impulsively started translating and spinning rotational symmetric body has been investigated by Ece [9] who obtained the solution for small values of times. The corresponding heat transfer problem has been considered by Ozturk and Ece [10]. In a most recent investigation, Takhar et al. [11] have presented a study on unsteady mixed convection flow over a vertical cone rotating in an ambient fluid with a time-dependent angular velocity in the presence of a magnetic field. Therefore, as a step towards the eventual development of studies on unsteady mixed
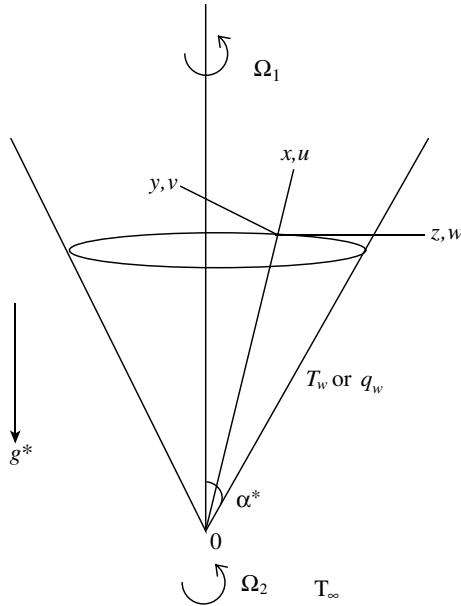
Fig. 1. Physical model and coordinate system.

convection flows, it is interesting as well as useful to investigate the combined effects of thermal and mass diffusion on a rotating cone in a rotating viscous fluid where the angular velocity of the cone and the free stream angular velocity vary arbitrarily with time.

The aim of the present study is to analyze the combined effects of thermal and mass diffusion on an unsteady mixed convection flow over a rotating cone in a corotating fluid. The unsteadiness in the flow field is due to angular velocity of the cone and the freestream angular velocity which vary arbitrarily with time. The semi-similar solution of the coupled non-linear partial differential equations governing the mixed convection flow has been obtained numerically using the method of quasi-linearization technique and an implicit finite difference scheme [12]. Particular cases of the present results have been compared with those of Hering and Grosh [5], Himasekhar et al. [6] and Takhar et al. [11].

2. Analysis

Consider the unsteady laminar mixed convection flow over an infinite rotating cone in a rotating viscous fluid. The unsteadiness in the flow field is introduced by rotating the cone and the surrounding free stream fluid about the axis of the cone with time-dependent angular velocities either in the same direction or in the opposite direction. Fig. 1 shows the coordinate system and the physical model. The buoyancy forces arise due to both the temperature and concentration variations in the fluid and the flow is taken to be axisymmetric. Both the

temperature and concentration at the wall vary linearly with the tangential coordinate x. Under the above assumptions and using the Boussinesq approximation, the governing boundary layer momentum, energy and diffusion equations can be expressed as [6,11,13,14]

$$(xu)_x + (xw)_z = 0, \tag{1}$$

$$u_t + uu_x + wu_z - \frac{v^2}{x} = -\frac{v_e^2}{x} + vu_{zz} + g^*\beta\cos\alpha^*(T - T_\infty)$$
$$+ g^*\beta^*\cos\alpha^*(C - C_\infty), \tag{2}$$

$$v_t + uv_x + wv_z + \frac{uv}{x} = (v_e)_t + vv_{zz}, \tag{3}$$

$$T_t + uT_x + wT_z = \alpha T_{zz}, \tag{4}$$

$$C_t + uC_x + wC_z = DC_{zz}. \tag{5}$$

The initial conditions are

$$u(0,x,z) = u_i(x,z), \quad v(0,x,z) = v_i(x,z),$$
$$w(0,x,z) = w_i(x,z), \quad T(0,x,z) = T_i(x,z),$$
$$C(0,x,z) = C_i(x,z), \tag{6}$$

and the boundary conditions are given by

$$u(t,x,0) = w(t,x,0) = 0, \quad v(t,x,0) = \Omega_1 x\sin\alpha^* R(t^*),$$
$$T(t,x,0) = T_w \text{ and } C(t,x,0) = C_w \quad \text{for PWT case,}$$
$$-kT_z(t,x,0) = q_w \text{ and } -\rho DC_z(t,x,0) = \dot{m}_w$$
$$\quad \text{for PHF case,}$$
$$u(t,x,\infty) = 0, \quad v(t,x,\infty) = v_e = \Omega_2 x\sin\alpha^* R(t^*),$$
$$T(t,x,\infty) = T_\infty, \quad C(t,x,\infty) = C_\infty. \tag{7}$$

Applying the following transformations for prescribed wall temperature (PWT) case

$$\eta = (\Omega\sin\alpha^*/v)^{\frac{1}{2}}z, \quad v_e = \Omega_2 x\sin\alpha^* R(t^*), \quad \Omega = \Omega_1 + \Omega_2,$$
$$t^* = (\Omega\sin\alpha^*)t, \quad u(t,x,z) = -2^{-1}\Omega x\sin\alpha^* R(t^*)f_\eta(\eta,t^*),$$
$$v(t,x,z) = \Omega x\sin\alpha^* R(t^*)g(\eta,t^*),$$
$$w(t,x,z) = (v\Omega\sin\alpha^*)^{\frac{1}{2}}R(t^*)f(\eta,t^*),$$
$$T(t,x,z) - T_\infty = (T_w - T_\infty)\theta(\eta,t^*),$$
$$T_w - T_\infty = (T_0 - T_\infty)\left(\frac{x}{L}\right),$$
$$C(t,x,z) - C_\infty = (C_w - C_\infty)\phi(\eta,t^*),$$
$$C_w - C_\infty = (C_0 - C_\infty)\left(\frac{x}{L}\right),$$
$$Gr_1 = g^*\beta\cos\alpha^*(T_0 - T_\infty)\frac{L^3}{v^2}, \quad Re_L = \Omega\sin\alpha^*\frac{L^2}{v}, \quad \lambda_1 = \frac{Gr_1}{Re_L^2},$$
$$Gr_2 = g^*\beta^*\cos\alpha^*(C_0 - C_\infty)\frac{L^3}{v^2}, \quad \lambda_2 = \frac{Gr_2}{Re_L^2},$$
$$R(t^*) = 1 + \epsilon t^{*2}, \quad \alpha_1 = \frac{\Omega_1}{\Omega}, \quad N = \frac{\lambda_2}{\lambda_1}, \quad Pr = \frac{v}{\alpha}, \quad Sc = \frac{v}{D},$$
$$\tag{8}$$

and for the prescribed heat flux (PHF) case:

$$\eta = (\Omega \sin\alpha^* / v)^{\frac{1}{2}} z, \quad v_e = \Omega_2 x \sin\alpha^* R(t^*),$$

$$t^* = (\Omega \sin\alpha^*) t, \quad u(t,x,z) = -2^{-1} \Omega x \sin\alpha^* R(t^*) F_\eta(\eta, t^*),$$

$$v(t,x,z) = \Omega x \sin\alpha^* R(t^*) G(\eta, t^*),$$

$$w(t,x,z) = (v \Omega \sin\alpha^*)^{\frac{1}{2}} R(t^*) F(\eta, t^*),$$

$$T(t,x,z) - T_\infty = (\Omega \sin\alpha^* / v)^{-\frac{1}{2}} \left(\frac{q_w}{k}\right) \Theta(\eta, t^*), \quad q_w = q_0 \left(\frac{x}{L}\right),$$

$$C(t,x,z) - C_\infty = (\Omega \sin\alpha^* / v)^{-\frac{1}{2}} \left(\frac{\dot{m}_w}{\rho D}\right) \Phi(\eta, t^*), \quad \dot{m}_w = \dot{m}_0 \left(\frac{x}{L}\right),$$

$$Gr_1^* = \frac{g^* \beta \cos\alpha^* q_0 L^4}{k v^2}, \quad \lambda_1^* = \frac{Gr_1^*}{Re_L^{\frac{5}{2}}}, \quad \alpha_1 = \frac{\Omega_1}{\Omega}, \quad N^* = \frac{\lambda_2^*}{\lambda_1^*},$$

$$Gr_2^* = \frac{g^* \beta^* \cos\alpha^* (\dot{m}_0) L^4}{\rho D v^2}, \quad \lambda_2^* = \frac{Gr_2^*}{Re_L^{\frac{5}{2}}}, \quad Pr = \frac{v}{\alpha}, \quad Sc = \frac{v}{D},$$

$$(9)$$

to Eqs. (1)–(5), we find that Eq. (1) is identically satisfied, and Eqs. (2)–(5) for the prescribed wall temperature (PWT) case reduce to

$$f_{\eta\eta\eta} - R(t^*) f f_{\eta\eta} + 2^{-1} R(t^*) f_\eta^2 - 2R(t^*)[g^2 - (1 - \alpha_1)^2]$$

$$- 2R(t^*)^{-1} \lambda_1 (\theta + N\phi) - R(t^*)^{-1} \left(\frac{dR}{dt^*}\right) f_\eta - f_{\eta t^*} = 0,$$

$$(10)$$

$$g_{\eta\eta} - R(t^*)[f g_\eta - g f_\eta] - R(t^*)^{-1} \left(\frac{dR}{dt^*}\right)[g - (1 - \alpha_1)]$$

$$- g_{t^*} = 0, \quad (11)$$

$$Pr^{-1} \theta_{\eta\eta} - R(t^*) \left(f\theta_\eta - f_\eta \frac{\theta}{2}\right) - \theta_{t^*} = 0, \quad (12)$$

$$Sc^{-1} \phi_{\eta\eta} - R(t^*) \left[f\phi_\eta - f_\eta \frac{\phi}{2}\right] - \phi_{t^*} = 0, \quad (13)$$

and for prescribed heat flux (PHF) case, the equations corresponding to Eqs. (10)–(13) are given by

$$F_{\eta\eta\eta} - R(t^*) F F_{\eta\eta} + 2^{-1} R(t^*) F_\eta^2 - 2R(t^*)[G^2 - (1 - \alpha_1)^2]$$

$$- 2R(t^*)^{-1} \lambda_1^* (\Theta + N^* \Phi) - R(t^*)^{-1} \left(\frac{dR}{dt^*}\right) F_\eta$$

$$- F_{\eta t^*} = 0, \quad (14)$$

$$G_{\eta\eta} - R(t^*)[F G_\eta - G F_\eta] - R(t^*)^{-1} \left(\frac{dR}{dt^*}\right)[G - (1 - \alpha_1)]$$

$$- G_{t^*} = 0, \quad (15)$$

$$Pr^{-1} \Theta_{\eta\eta} - R(t^*) \left(F\Theta_\eta - F_\eta \frac{\Theta}{2}\right) - \Theta_{t^*} = 0, \quad (16)$$

$$Sc^{-1} \Phi_{\eta\eta} - R(t^*) \left[F\Phi_\eta - F_\eta \frac{\Phi}{2}\right] - \Phi_{t^*} = 0. \quad (17)$$

The boundary conditions for the PWT case are given by

$$f(0,t^*) = 0 = f_\eta(0,t^*), \quad g(0,t^*) = \alpha_1,$$

$$\theta(0,t^*) = \phi(0,t^*) = 1, \quad f_\eta(\infty,t^*) = 0,$$

$$g(\infty,t^*) = 1 - \alpha_1, \quad \theta(\infty,t^*) = \phi(\infty,t^*) = 0. \quad (18)$$

The boundary conditions for the PHF case are expressed by

$$F(0,t^*) = 0 = F_\eta(0,t^*), \quad G(0,t^*) = \alpha_1,$$

$$\Theta_\eta(0,t^*) = \Phi_\eta(0,t^*) = -1, \quad F_\eta(\infty,t^*) = 0,$$

$$G(\infty,t^*) = 1 - \alpha_1, \quad \Theta(\infty,t^*) = \Phi(\infty,t^*) = 0. \quad (19)$$

It may be remarked that, $\alpha_1 = 0$ implies that the cone is stationary and the fluid is rotating, $\alpha_1 = 1$ represents the case where the cone is rotating in an ambient fluid, and for $\alpha_1 = 0.5$, the cone and the free stream fluid are rotating with equal angular velocity in the same direction. Thus, for the case $\alpha_1 < 0.5$, $\Omega_1 < \Omega_2$ and for $\alpha_1 > 0.5$, $\Omega_1 > \Omega_2$. Further for $\alpha_1 < 0$, the cone and the free stream fluid are rotating in the opposite direction. The ratio of Grashof numbers denoted by the parameter N(PWT case) or N^* (PHF case) measures the relative importance of thermal and mass diffusion in inducing the buoyancy forces which drive the flow. N or $N^* = 0$ for no species diffusion, infinite for the thermal diffusion, positive for the case when the buoyancy forces due to temperature and concentration difference act in the same direction and negative when they act in the opposite direction.

We have assumed that the flow is steady at time $t^* = 0$ and becomes unsteady for $t^* > 0$ due to the time-dependent angular velocities ($R(t^*) = 1 + \epsilon t^{*2}, \epsilon \lessgtr 0$) of the cone and the free stream fluid. Hence, the initial conditions (i.e., conditions at $t^* = 0$) are given by the steady state equations obtained from Eqs. (10)–(17) by substituting $R(t^*) = 1$, $\frac{dR}{dt^*} = f_{\eta t^*} = g_{t^*} = \theta_{t^*} = \phi_{t^*} = 0$ and $F_{\eta t^*} = G_{t^*} = \Theta_{t^*} = \Phi_{t^*} = 0$ when $t^* = 0$. The corresponding boundary conditions for PWT and PHF cases are obtained from (18) and (19), respectively when $t^* = 0$.

It may be noted that the steady state equations in the absence of mass diffusion for $\alpha_1 = 1$ and $N = 0$ of PWT case are the same as those of Hering and Grosh [5], and Himasekhar et al. [6]. Further, the unsteady Eqs. (10)–(12) in the absence of mass diffusion (i.e., without the species Eq. (13)) for $\alpha_1 = 1$ and $N = 0$ of the PWT case are the same for $M = 0$ case (i.e., in the absence of magnetic field) of Takhar et al. [11] who investigated recently an unsteady mixed convection flow from a rotating vertical cone with a magnetic field.

The quantities of physical interest are as follows [13,14]:

The local surface skin friction coefficients in x- and y-directions for the PWT case are, respectively given by

$$C_{fx} = \frac{\left[2\mu\left(\frac{\partial u}{\partial z}\right)\right]_{z=0}}{\rho[\Omega x \sin \alpha^*]^2} = -Re_x^{-\frac{1}{2}} R(t^*) f_{\eta\eta}(0, t^*),$$

$$C_{fy} = -\frac{\left[2\mu\left(\frac{\partial v}{\partial z}\right)\right]_{z=0}}{\rho[\Omega x \sin \alpha^*]^2} = -2Re_x^{-\frac{1}{2}} R(t^*) g_{\eta}(0, t^*).$$

Thus,

$$Re_x^{\frac{1}{2}} C_{fx} = -R(t^*) f_{\eta\eta}(0, t^*),$$
$$2^{-1} Re_x^{\frac{1}{2}} C_{fy} = -R(t^*) g_{\eta}(0, t^*), \tag{20}$$

where $Re_x = \Omega x^2 \sin \alpha^* / \nu$. Similarly, the local surface skin friction coefficients in x- and y-directions for PHF case are, respectively given by

$$Re_x^{\frac{1}{2}} \overline{C}_{fx} = -R(t^*) F_{\eta\eta}(0, t^*),$$
$$2^{-1} Re_x^{\frac{1}{2}} \overline{C}_{fy} = -R(t^*) G_{\eta}(0, t^*). \tag{21}$$

The local Nusselt number and local Sherwood number for the PWT case can be expressed as

$$Re_x^{-\frac{1}{2}} Nu_x = -\theta_{\eta}(0, t^*), \quad Re_x^{-\frac{1}{2}} Sh_x = -\phi_{\eta}(0, t^*), \tag{22}$$

where

$$Nu_x = -\frac{\left[x\left(\frac{\partial T}{\partial z}\right)\right]_{z=0}}{T_w - T_\infty} \quad \text{and} \quad Sh_x = -\frac{\left[x\left(\frac{\partial C}{\partial z}\right)\right]_{z=0}}{C_w - C_\infty}.$$

Similarly, the local Nusselt and Sherwood numbers for the PHF case are, respectively given in the form

$$Re_x^{-\frac{1}{2}} \overline{Nu_x} = \frac{1}{\Theta(0, t^*)}, \quad Re_x^{-\frac{1}{2}} \overline{Sh_x} = \frac{1}{\Phi(0, t^*)}. \tag{23}$$

3. Method of solution

The set of dimensionless Eqs. (10)–(13)—under the boundary conditions (18) for PWT case (Eqs. (14)–(17) under the boundary conditions (19) for PHF case) with the initial conditions obtained from the corresponding steady state equations has been solved numerically using an implicit finite difference scheme in combination with the quasi-linearization technique. Since the method is described by Inouye and Tate [12] and also explained in a recent article by Roy and Saikrishnan [15], its detailed description is not presented here for the sake of brevity. In brief, the non-linear coupled partial differential equations were replaced by an iterative sequence of linear equations following quasi-linearization technique. The resulting sequence of linear partial differential equations were expressed in difference form using central difference scheme in η-direction and backward difference scheme in t^*-direction. In each iteration step, the equations were then reduced to a system of linear algebraic equations with a block tri-diagonal structure which is solved by using Varga algorithm [16].

To ensure the convergence of the numerical solution to exact solution, the step sizes $\Delta\eta$ and Δt^* have been optimized and the results presented here are independent of the step sizes at least up to the fourth decimal place. The step sizes $\Delta\eta$ and Δt^* have been taken as 0.01 and 0.02, respectively. A convergence criteria based on the relative difference between the current and previous iteration values are employed. When the difference reaches less than 10^{-4}, the solution is assumed to have converged and the iterative process is terminated.

4. Results and discussion

The computations have been carried out for various values of Pr $(0.7 \leqslant Pr \leqslant 7.0)$, λ_1 $(0 \leqslant \lambda_1 \leqslant 5)$, α_1 $(-0.25 \leqslant \alpha_1 \leqslant 1.0)$, Sc $(0.22 \leqslant Sc \leqslant 2.57)$, N $(-0.5 \leqslant N \leqslant 1.0)$, λ_1^* $(0 \leqslant \lambda_1^* \leqslant 5)$ and N^* $(-0.5 \leqslant N^* \leqslant 1.0)$. The edge of the boundary layer η_∞ is taken between 4 and 6 depending on the values of parameters. The results have been obtained for both increasing $(R(t^*) = 1 + \epsilon t^{*2}$, $\epsilon = 0.2$, $0 \leqslant t^* \leqslant 2)$ and decreasing $(R(t^*) = 1 + \epsilon t^{*2}$, $\epsilon = -0.15$, $0 \leqslant t^* \leqslant 2)$ angular velocity of the cone and the free stream fluid. In order to validate our method, we have compared steady state results of skin-friction and heat transfer coefficients $(-f_{\eta\eta}(0,0), -g_{\eta}(0,0), -\theta_{\eta}(0,0))$ for PWT case with those of Hering and Grosh [5] and Himasekhar et al. [6]. The results are found in excellent agreement. We have also compared the skin friction and heat transfer coefficients $(-f_{\eta\eta}(0,t^*), -g_{\eta}(0,t^*), -\theta_{\eta}(0,t^*))$ for PWT case in the absence of mass diffusion $(N = 0)$ with the results of Takhar et al. [11] for $M = 0$, who studied recently the unsteady mixed convection flow from a rotating vertical cone with a magnetic field and found them in excellent agreement. Some of the comparisons are shown in Table 1 and Fig. 2.

The results for the prescribed wall temperature (PWT) case are presented in Figs. 3–11 and for the prescribed heat flux (PHF) case in Fig. 12.

The effects of the buoyancy parameter λ_1 and the parameter α_1 (which is the ratio of the angular velocity of the cone to the composite angular velocity) on the velocity, temperature and concentration profiles $(-f_\eta, g, \theta, \phi)$ are displayed in Figs. 3–5 for $R(t^*) = 1 + \epsilon t^{*2}$, $\epsilon = 0.2$, $t^* = 1$, $N = 1$, $Sc = 0.94$ and $Pr = 0.7$. Also, the effects of λ_1 and α_1 on the local skin friction coefficients $(Re_x^{1/2} C_{fx}, 2^{-1} Re_x^{1/2} C_{fy})$ and the local Nusselt and Sherwood numbers $(Re_x^{-1/2} Nu_x, Re_x^{-1/2} Sh_x)$ are presented in Figs. 6 and 7. It is observed from Figs. 3 and 4 that the ratio of angular velocities α_1 strongly affects the velocity profiles $(-f_\eta, g)$. For $\alpha_1 = 0.5$, the cone and the fluid are rotating with equal angular velocity in the same direction and the non-zero velocities in tangential and azimuthal directions $(-f_\eta, g)$ for $\alpha_1 = 0.5$ are only due to the positive buoyancy parameter $\lambda_1 = 1$, which acts like a favourable pressure gradient. When $\alpha_1 > 0.5$, the fluid

Table 1
Comparison of the steady state results $(f''(0), -s'(0), -\theta'(0))$ with those of Hering and Grosh [5] and Himasekhar et al. [6]

Pr	λ_1	Present results			Himasekhar et al. [6]		
		$-\theta'(0)$	$-g'(0)$	$-f''(0)$	$-\theta'(0)$	$-g'(0)$	$-f''(0)$
0.7	1	0.6127	0.8499	2.1757	0.6120	0.8496	2.2012
		0.6120[a]	0.8507[a]	2.2078[a]			
	10	1.0175	1.4061	8.5029	1.0097	1.3990	8.5041
		1.0173[a]	1.4037[a]	8.5246[a]			
1	1	0.7005	0.8250	2.0627	0.7010	0.8176	2.0886
	10	1.1494	1.3504	7.9045	1.1230	1.3460	7.9425
10	1	1.5885	0.6894	1.5458	1.5662	0.6837	1.5636
	10	2.3582	0.9903	5.0531	2.3580	0.9840	5.0821

[a] Values taken from Hering and Grosh [5].
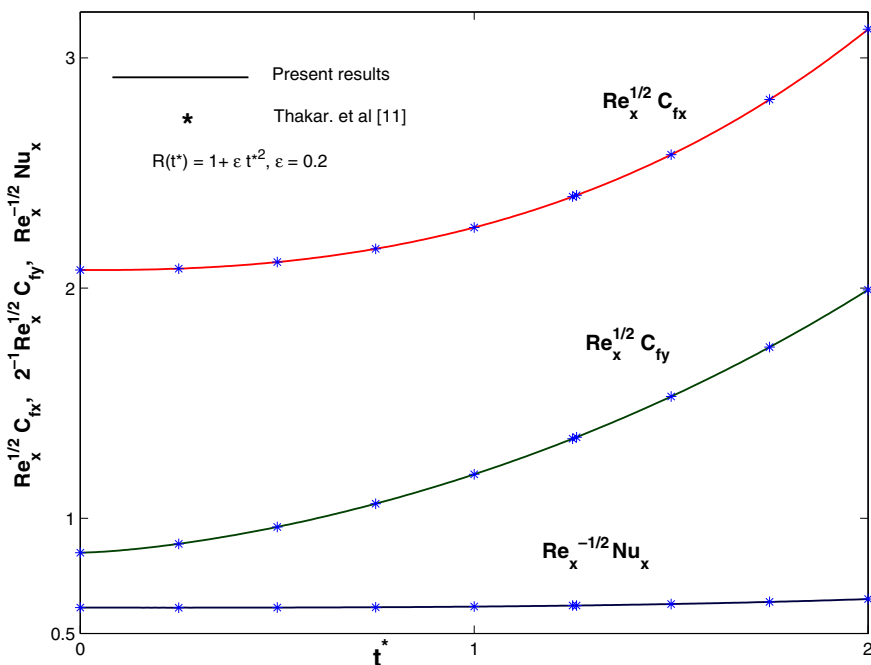
Fig. 2. Comparisons of skin friction and heat transfer coefficients with those of Takhar et al. [11] for PWT case when $Pr = 0.7$, $\lambda_1 = 1$, $N = 0$ and $\alpha_1 = 1$.

is being dragged by the rotating cone and due to the combined effects of buoyancy force and rotation, the tangential velocity $(-f_\eta)$ increases its magnitude but the azimuthal velocity (g) decreases its magnitude within the boundary layer. On the other hand, when $\alpha_1 < 0.5$, the cone is dragged by the fluid and the combined effects of buoyancy force and rotation parameter is just the opposite. Since the positive buoyancy force $(\lambda_1 > 0)$ implies favourable pressure gradient, the fluid gets accelerated which results in thinner momentum, thermal and concentration boundary layers. Consequently, the velocity, temperature and concentration gradients are

increased (see Figs. 3–5). Hence, the local skin friction coefficients $(Re_x^{1/2}C_{fx}, 2^{-1}Re_x^{1/2}C_{fy})$ and the local Nusselt and Sherwood numbers $(Re_x^{-1/2}Nu_x, Re_x^{-1/2}Sh_x)$ are also increased at any time t^* as shown in Figs. 6 and 7. For example, $\alpha_1 = 0.75$ at time $t^* = 1$, Figs. 6 and 7 show that the percentage increase in $Re_x^{1/2}C_{fx}$, $2^{-1}Re_x^{1/2}C_{fy}$, $Re_x^{-1/2}Nu_x$ and $Re_x^{-1/2}Sh_x$ due to the increase in λ_1 from 1 to 3 are about 111%, 28%, 33% and 27%, respectively. The effect of the time variation is found to be more pronounced on the skin friction coefficients $(Re_x^{1/2}C_{fx}, 2^{-1}Re_x^{1/2}C_{fy})$ than on the Nusselt and Sherwood numbers $(Re_x^{-1/2}Nu_x, Re_x^{-1/2}Sh_x)$ because the change in the angular
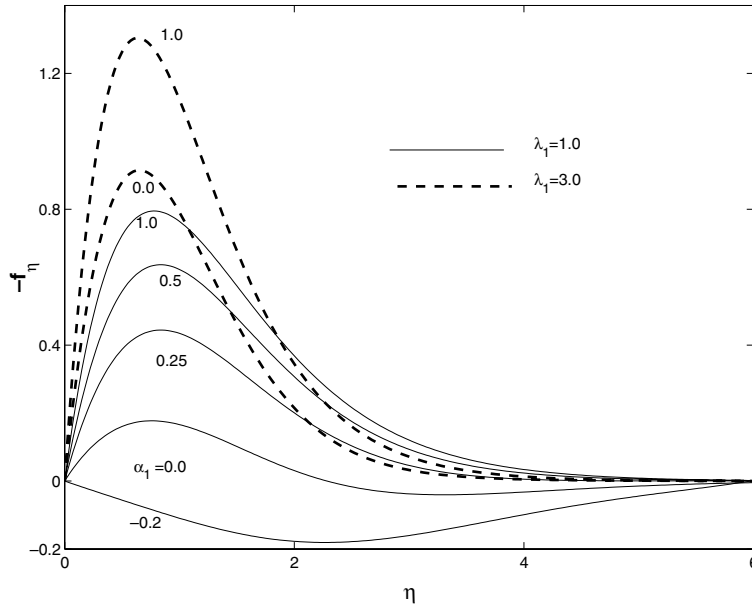
Fig. 3. Effects of α_1 and λ_1 on velocity profile $(-f_\eta)$ for PWT case with $N = 1$, $Pr = 0.7$, $Sc = 0.94$ when $R(t^*) = 1 + \epsilon t^2$, $\epsilon = 0.2$ at $t^* = 1$.
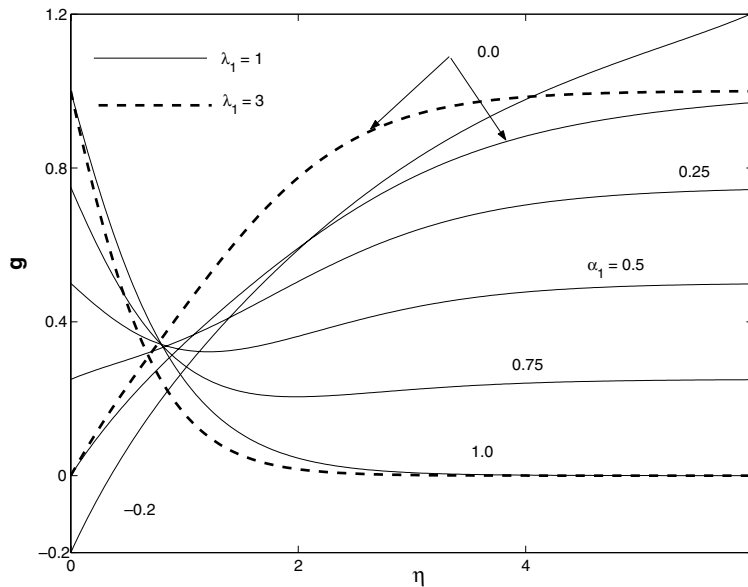
Fig. 4. Effects of α_1 and λ_1 on velocity profile (g) for PWT case with $N = 1$, $Pr = 0.7$, $Sc = 0.94$ when $R(t^*) = 1 + \epsilon t^2$, $\epsilon = 0.2$ at $t^* = 1$.

velocity with time strongly affect the velocity components. To be more specific for $\lambda_1 = 1$, $\alpha_1 = 1$, $N = 1$, the values of $Re_x^{1/2}C_{fx}$ and $2^{-1}Re_x^{1/2}C_{fy}$ increase by about 20% and 103%, respectively when the time t^* increases from 0 to 2. On the other hand for the same data, $Re_x^{-1/2}Nu_x$ and $Re_x^{-1/2}Sh_x$ increase approximately by 3% and 4%, respectively for the increase of t^* from 0 to 2.

Figs. 8 and 9 display the effect of the ratio of the buoyancy forces N (which measures the relative importance of the species and thermal diffusion) on the local skin friction coefficients $(Re_x^{1/2}C_{fx}, 2^{-1}Re_x^{1/2}C_{fy})$ and the local Nusselt and Sherwood numbers $(Re_x^{-1/2}Nu_x, Re_x^{-1/2}Sh_x)$ for increasing and decreasing angular velocities $(R(t^*) = 1 + \epsilon t^{*2}$, $\epsilon = 0.2$ and $\epsilon = -0.15)$ when
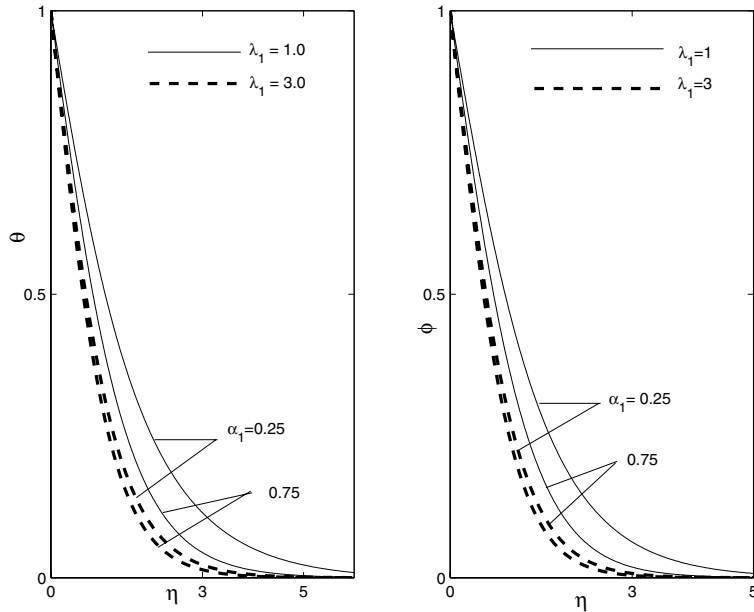
Fig. 5. Effects of α_1 and λ_1 on temperature and concentration profiles (θ, ϕ), for PWT case with $N = 1$, $Pr = 0.7$, $Sc = 0.94$ when $R(t^*) = 1 + \epsilon t^2$, $\epsilon = 0.2$ at $t^* = 1$.
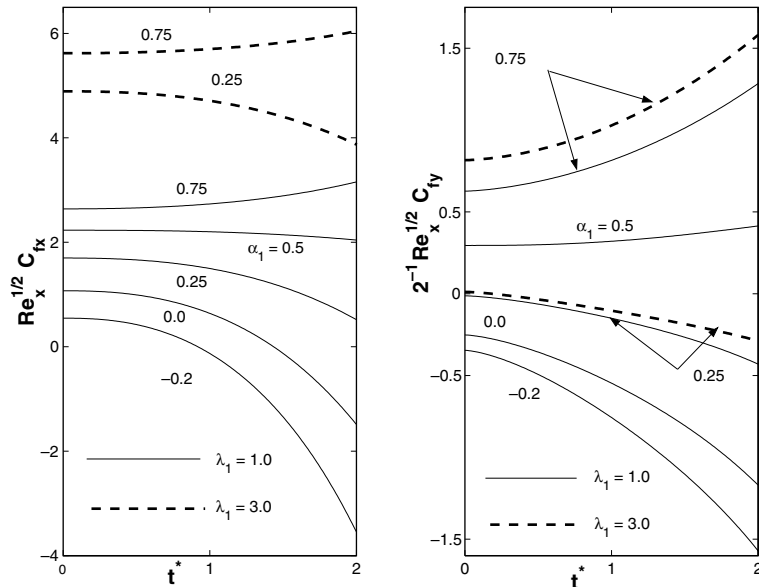
Fig. 6. Effects of α_1 and λ_1 on $Re_x^{1/2}C_{fx}$ and $2^{-1}Re_x^{1/2}C_{fy}$ for PWT case with $N = 1$, $Pr = 0.7$, $Sc = 0.94$ when $R(t^*) = 1 + \epsilon t^2$, $\epsilon = 0.2$.

$\lambda_1 = 1$, $\alpha_1 = 0.75$, $Pr = 0.7$ and $Sc = 0.94$. Due to the increase in N, the velocity gradient in the primary flow as well as in the secondary flow i.e., skin friction coefficients $(Re_x^{1/2}C_{fx}, 2^{-1}Re_x^{1/2}C_{fy})$ and the Nusselt and Sherwood numbers $(Re_x^{-1/2}Nu_x, Re_x^{-1/2}Sh_x)$ increase for both increasing $(\epsilon > 0)$ and decreasing $(\epsilon < 0)$ angular

velocity cases at any time t^*. For example, the percentage increase in $Re_x^{1/2}C_{fx}$, $2^{-1}Re_x^{1/2}C_{fy}$, $Re_x^{-1/2}Nu_x$ and $Re_x^{-1/2}Sh_x$ due to the increase in N from -0.5 to 1 are about 100%, 25%, 29% and 28%, respectively for the increasing angular velocity case $(\epsilon = 0.2)$ at time $t^* = 1.0$. It is observed from Fig. 8 that for a fixed N, the skin
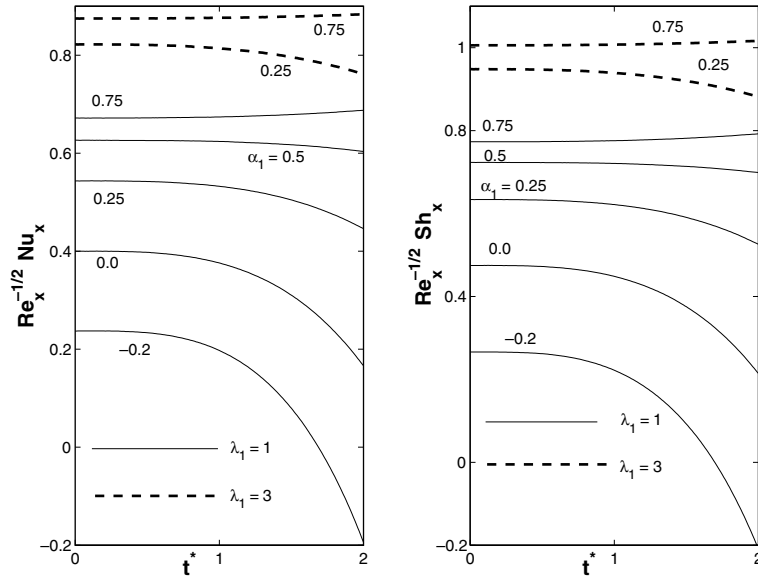
Fig. 7. Effects of α_1 and λ_1 on $Re_x^{-1/2}Nu_x$ and $Re_x^{-1/2}Sh_x$ for PWT case with $N = 1$, $Pr = 0.7$, $Sc = 0.94$ when $R(t^*) = 1 + \epsilon t^2$, $\epsilon = 0.2$.
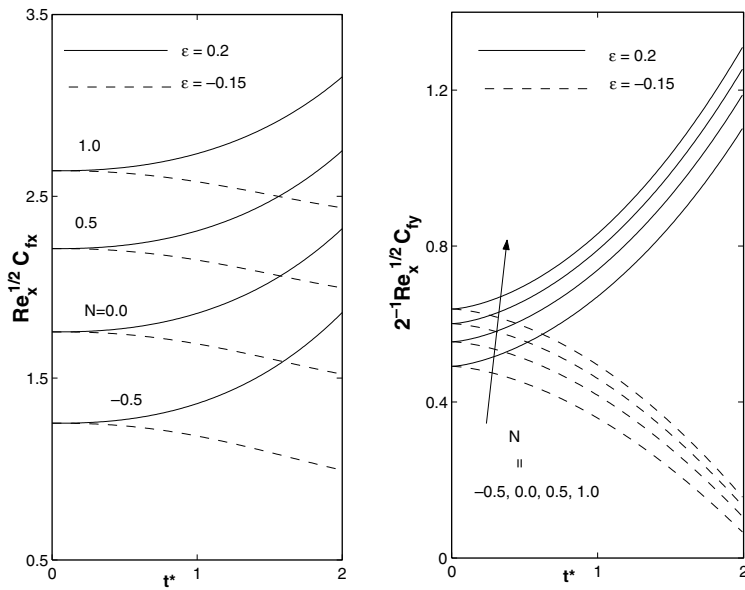
Fig. 8. Effect of N on $Re_x^{1/2}C_{fx}$ and $2^{-1}Re_x^{1/2}C_{fy}$ for PWT case with $\alpha_1 = 0.75$, $\lambda_1 = 1$, $Pr = 0.7$, $Sc = 0.94$ when $R(t^*) = 1 + \epsilon t^2$, $\epsilon = 0.2$ and $\epsilon = -0.15$.

friction coefficients increase with time t^* for an increasing angular velocity but for decreasing angular velocity, the trend is reverse. For example, for increasing angular velocity with $N = 0.5$ and $\epsilon = 0.2$, $Re_x^{1/2}C_{fx}$ and $2^{-1}Re_x^{1/2}C_{fy}$ increase approximately by 25% and 107%, respectively as the time t^* increases from 0 to 2. But for a decreasing angular velocity with $N = 0.5$ and $\epsilon = -0.15$,

$Re_x^{1/2}C_{fx}$ and $2^{-1}Re_x^{1/2}C_{fy}$ decrease approximately by 10% and 78%, respectively as the time t^* increases from 0 to 2. Since an increase in the angular velocity with time directly affects the tangential and azimuthal velocity components, the skin friction coefficients are significantly affected. However, the effect of an increase in the angular velocity on the energy and species equations are
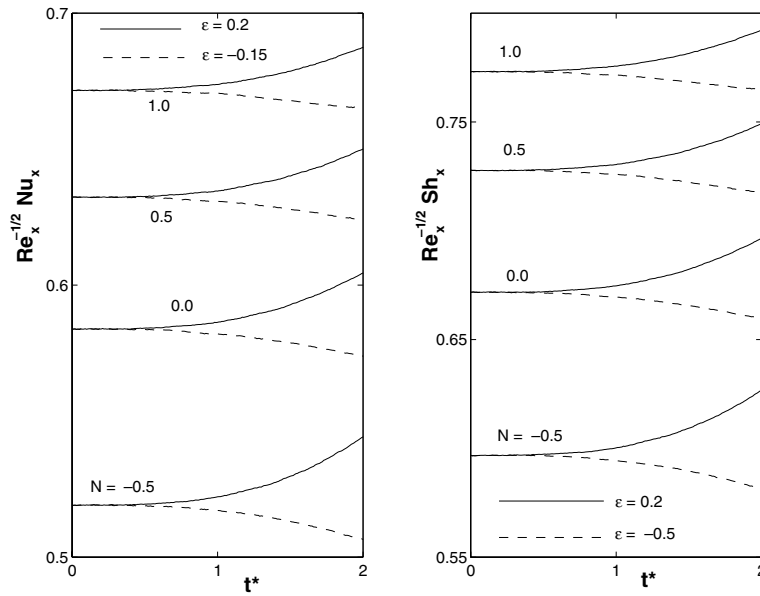
Fig. 9. Effect of N on $Re_x^{-1/2}Nu_x$ and $Re_x^{-1/2}Sh_x$ for PWT case with $\alpha_1 = 0.75$, $\lambda_1 = 1$, $Pr = 0.7$, $Sc = 0.94$ when $R(t^*) = 1 + \epsilon t^2$, $\epsilon = 0.2$ and $\epsilon = -0.15$.
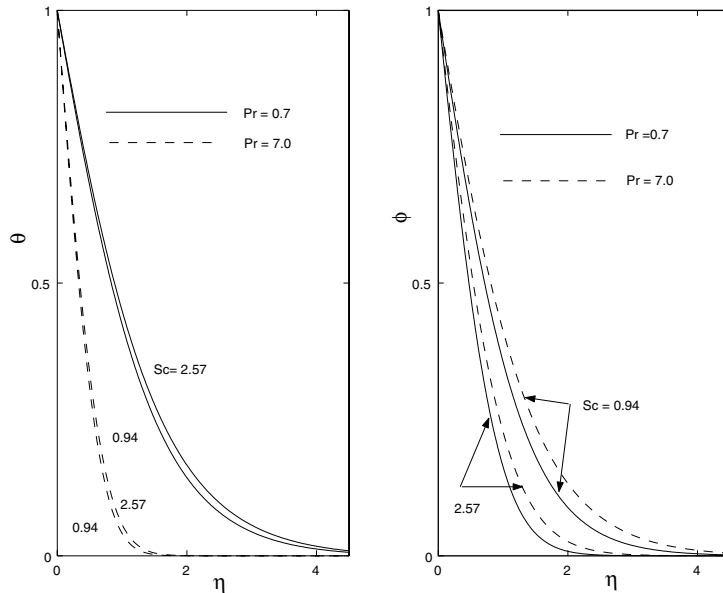
Fig. 10. Effects of Pr and Sc on θ and ϕ for PWT case with $N = 1$, $\alpha_1 = 0.75$, $\lambda_1 = 1$ when $R(t^*) = 1 + \epsilon t^2$, $\epsilon = 0.2$ at $t^* = 1$.

rather indirect. Hence, the local Nusselt and Sherwood numbers $(Re_x^{-1/2}Nu_x, Re_x^{-1/2}Sh_x)$ are weakly affected. In fact, the changes in the values of $Re_x^{-1/2}Nu_x$ and $Re_x^{-1/2}Sh_x$ for an increasing/decreasing angular velocity are within 3% as the time t^* increases from 0 to 2, which are displayed in Fig. 9.

The effects of Pr and Sc on the temperature and the concentration profiles (θ, ϕ) for increasing angular velocity $(R(t^*) = 1 + \epsilon t^{*2}, \epsilon = 0.2)$ when $\lambda_1 = 1$, $N = 1.0$ and $\alpha_1 = 0.75$ are presented in Fig. 10. Also, the effects of Pr and Sc on the local Nusselt and Sherwood numbers $(Re_x^{-1/2}Nu_x, Re_x^{-1/2}Sh_x)$ for the same data are shown in
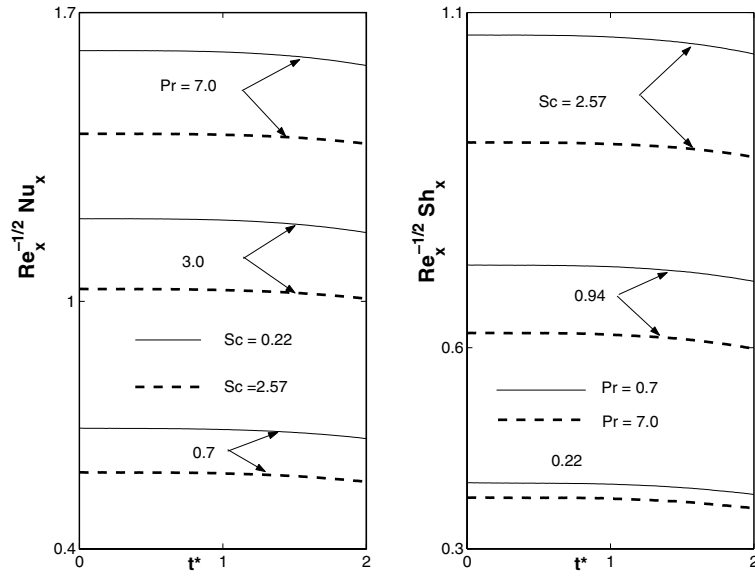
Fig. 11. Effects of Pr and Sc on $Re_x^{-1/2}Nu_x$ and $Re_x^{-1/2}Sh_x$ for PWT case with $N = 1$, $\alpha_1 = 0.75$, $\lambda_1 = 1$ when $R(t^*) = 1 + \epsilon t^2$, $\epsilon = 0.2$.
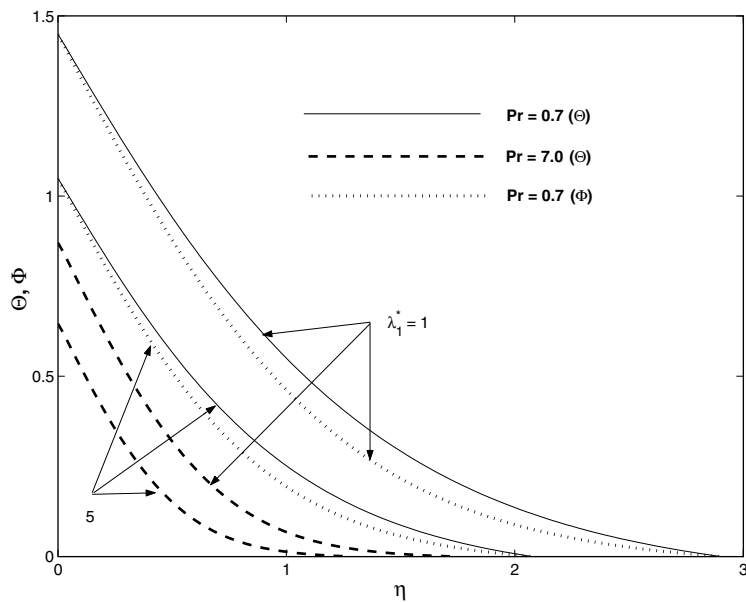
Fig. 12. Effects of λ_1^* and Pr on Θ and Φ for PHF case with $N^* = 1$, $\alpha_1 = 0.75$, $Sc = 0.94$ when $R(t^*) = 1 + \epsilon t^2$, $\epsilon = 0.2$ at $t^* = 1$.

Fig. 11. The temperature and concentration profiles in Fig. 10 reveal the fact that the thermal boundary layer thickness increases rapidly with decreasing Pr and the concentration boundary layer thickness increases significantly with decreasing Sc. Hence in Fig. 11, $Re_x^{-1/2}Nu_x$ increases with Pr and $Re_x^{-1/2}Sh_x$ increases with Sc. For example, for $Sc = 0.22$, $Re_x^{-1/2}Nu_x$ increases by about 132% as Pr increases from 0.7 to 7.0 and for $Pr = 0.7$,

$Re_x^{-1/2}Sh_x$ increases by about 165% as Sc increases from 0.22 to 2.57. It may be remarked that the skin friction coefficients $(Re_x^{1/2}C_{fx}, 2^{-1}Re_x^{1/2}C_{fy})$ are less affected by Pr and Sc as compared to the Nusselt and Sherwood numbers $(Re_x^{-1/2}Nu_x, Re_x^{-1/2}Sh_x)$. In particular, for an increasing angular velocity $(R(t^*) = 1 + \epsilon t^{*2}, \epsilon = 0.2)$ at $t^* = 1$, when Pr changes from 0.7 to 7.0 the variations in the values of $Re_x^{1/2}C_{fx}$ and $2^{-1}Re_x^{1/2}C_{fy}$ are within 18%

and the variations are within 8% for the change of Sc from 0.22 to 2.57. Thus, the effects of Pr and Sc on the velocity profiles $(-f_\eta, g)$ and the skin friction coefficients $(Re_x^{1/2}C_{fx}, 2^{-1}Re_x^{1/2}C_{fy})$ are not presented here to limit the number of figures.

For the prescribed heat flux (PHF) case, the effects of buoyancy parameter λ_1^* and Prandtl number Pr on temperature and concentration profiles (Θ, Φ) for increasing angular velocity $(R(t^*) = 1 + \epsilon t^{*2}, \ \epsilon = 0.2)$ with $Sc = 0.94$, $N = 1$ and $\alpha_1 = 0.75$ are displayed in Fig. 12. Fig. 12 shows that unlike the PWT case where temperature and concentration profiles (θ, ϕ) vary from 1 on the wall to 0 at the edge of the boundary layer η_∞, in the PHF case temperature and concentration profiles (Θ, Φ) on the wall are different from 1. This behaviour is to be expected as the boundary conditions $\Theta_\eta(\eta, t^*) = \Phi_\eta(\eta, t^*) = -1$ on the wall (i.e., $\Theta_\eta(0, t^*) = \Phi_\eta(0, t^*) = -1$) are being imposed and all temperature and concentration profiles $\Theta(\eta)$ and $\Phi(\eta)$ are equally inclined to the vertical axis at $\eta = 0$ as shown in Fig. 12. It is observed from Fig. 12 that the thermal boundary layer thickness reduces significantly with the increase of Prandtl number Pr. The physical reason is that the higher Prandtl number fluid has a lower thermal conductivity which results in thinner thermal boundary layer. Since the structure of the equations in both the cases (PWT and PHF) are almost similar, it is natural to expect the effects of α_1, λ_1^*, N^* and Sc are to be similar in the present PHF case as in the PWT case and the results are therefore not presented here to reduce the number of figures.

5. Conclusions

Unsteady mixed convection flow on a rotating cone in a rotating fluid due to the combined effects of thermal and mass diffusion has been studied numerically to obtain semi-similar solutions fot both PWT and PHF conditions. The results have been obtained for increasing and decreasing angular velocity cases. Comparisons with previously published work on modified cases of the problem were performed and found to be in good agreement. The results indicate that skin friction coefficients in x- and y-directions change significantly with time but the change in Nusselt and Sherwood numbers are comparatively very small. It was found that the buoyancy force (λ_1 or λ_1^*) enhances the skin friction coefficients, Nusselt and Sherwood numbers. For a fixed buoyancy force, the Nusselt and Sherwood numbers increase with Prandtl number but the skin friction coefficients decrease. In fact, the increase in Prandtl number and Schmidt number causes a significant reduction in the thickness of thermal and concentration boundary layers, respectively. Due to the increase in the ratio of buoyancy forces (N), the skin friction coefficients, Nusselt and Sherwood numbers increase.

References

[1] S. Ostrach, W.H. Brown, Natural convection inside a flat rotating container. NACA TN 4323 (1958).
[2] C.L. Tien, I.J. Tsuji, A theoretical analysis of laminar forced flow and heat transfer about a rotating cone, ASME J. Heat Transfer 87 (1965) 184–190.
[3] T.C.Y Koh, J.F. Price, Nonsimilar boundary layer heat transfer of a rotating cone in forced flow, ASME J. Heat Transfer 89 (1967) 139–145.
[4] J.P. Hartnett, E.C. Deland, The influence of Prandtl number on the heat transfer from rotating non-isothermal disks and cones, ASME J. Heat Transfer 83 (1961) 95–96.
[5] R.G. Hering, R.J. Grosh, Laminar combined convection from a rotating cone, ASME J. Heat Transfer 85 (1963) 29–34.
[6] K. Himasekhar, P.K. Sarma, K. Janardhan, Laminar mixed convection from a vertical rotating cone, Int. Comm. Heat Mass Transfer 16 (1989) 99–106.
[7] C.Y. Wang, Boundary layers on rotating cones, discs and axisymmetric surfaces with a concentrated heat source, Acta Mech. 81 (1990) 245–251.
[8] K.A. Yih, Mixed convection about a cone in a porous medium: the entire regime, Int. Comm. Heat Mass Transfer 26 (1999) 1041–1050.
[9] M.C. Ece, An initial boundary layer flow past a translating and spinning rotational symmetric body, J. Eng. Math. 26 (1992) 415–428.
[10] A. Ozturk, M.C. Ece, Unsteady forced convection heat transfer from a translating and spinning body, ASME J. Heat Transfer 117 (1995) 318–323.
[11] H.S. Takhar, A.J. Chamkha, G. Nath, Unsteady mixed convection flow from a rotating vertical cone with a magnetic field, Heat Mass Transfer 39 (2003) 297–304.
[12] K. Inouye, A. Tate, Finite difference version quasilinearization applied to boundary layer equations, AIAAJ 12 (1974) 558–560.
[13] I. Pop, D.B. Ingham, Convective Heat Transfer: Mathematical and Computational Modelling of Viscous Fluids and Porous Media, Pergaman, Oxford, 2001.
[14] A. Bejan, Convective Heat Transfer, Wiley Interscience, 1994.
[15] S. Roy, P. Saikrishnan, Non-uniform slot injection (suction) into steady laminar water boundary layer flow over a rotating sphere, Int. J. Heat Mass Transfer 46 (2003) 3389–3396.
[16] R.S. Varga, Matrix Iterative Analysis, Prentice Hall, 2000.